Organic & Biomolecular Chemistry

ROYAL SOCIETY OF CHEMISTRY

COMMUNICATION

View Article Online
View Journal | View Issue

Cite this: *Org. Biomol. Chem.*, 2020, **18**, 5334

Received 12th June 2020,
Accepted 22nd June 2020

DOI: 10.1039/d0ob01213k

rsc.li/obc

Deprotection of a benzyl unit induces a 22π aromatic macrocycle of 3-oxypyripentaphyrin (0.1.1.1.0) with strong NIR absorption†

Daiki Mori,[a] Tomoki Yoneda, *[a,b] Masaaki Suzuki,[c] Tyuji Hoshino [a] and Saburo Neya*[a]

We report aromaticity switching from a 6π pyridine ring to a 22π macrocyclic ring of 3-oxypyripentaphyrin(0.1.1.1.0). This system has potential applications in photodynamic therapy owing to macrocyclic aromaticity being selectively induced by protecting group removal and strong absorption bands produced in the NIR region especially in methanol.

Porphyrins and their analogs are employed for photodynamic therapy (PDT), which is a treatment used to eliminate cancer or abnormal tissue lesions.[1] Conventional porphyrin photosensitisers have their longest absorption maxima in the visible-light range. However, regarding penetration depth, a photosensitiser with absorbance in the NIR region (700–1100 nm) is desired.[2] Expanded porphyrins with large π-conjugation circuits[3] which absorb light reaching the NIR region are expected for applications in photodynamic therapy.[4] However, a known undesirable side effect of the existing photosensitisers is phototoxicity toward healthy tissues. This problem can be more serious when expanded porphyrins with strong absorption in the visible and NIR regions are adopted as photosensitisers. If the strong NIR absorption of a molecule is induced by deprotection, this system can be a photosensitizer candidate. This system prevents photosensitivity toward ambient light until metabolization occurs in tumors or tissue lesions. The removal of the protecting group is theoretically applicable to new reagents for NIR photodynamic therapy by employing appropriate protecting groups metabolised in tumours. If the aromaticity of expanded porphyrins could also be triggered by metabolization, the molecule would show strong NIR absorption and a theoretically crucial candidate for photodynamic therapy would be obtained (Fig. 1).

As an example of such expanded porphyrin systems, we herein report an expanded porphyrin with macrocyclic aromaticity which is triggered by simple benzyl group deprotection. We designed the deprotection of 3-benzyloxypyripentaphyrin(0.1.1.1.0) **1** to produce 3-oxypyripentaphyrin(0.1.1.1.0) **2** as an expanded porphyrin system with the 3-oxypyridine ring (Scheme 1). The reported pentaphyrin(1.1.1.0.0)s with five pyrrole rings are known to have an aromatic character derived from their 22π conjugation circuits.[5] To improve the stability of such electron-rich pentaphyrins, we suggested installing a pyridine ring instead of pyrrole. Compared with pyrrole, in which 6π-electrons are delocalised on five atoms, the pyridine ring is more electron deficient because of delocalisation of the

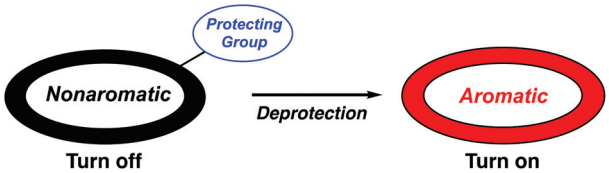

Fig. 1 Representation of the "deprotection induced aromaticity" strategy.

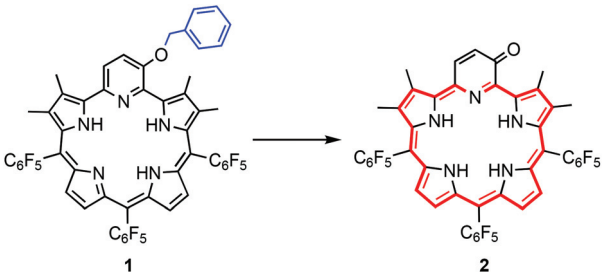

Scheme 1 Aromaticity induced by deprotection of **1**.

[a]*Department of Pharmaceutical Sciences, Chiba University, Inohana, Chuo-ku, Chiba, 260-8675, Japan*
[b]*Division of Applied Chemistry, Faculty of Engineering, Hokkaido University, Kita 13 Nishi 8 Kita-ku, Sapporo, Hokkaido, 060-8628, Japan.*
E-mail: t_yoneda@eng.hokudai.ac.jp
[c]*Graduate School of Natural Science and Technology, Shimane University, 1060, Nishikawatsu-cho, Matsue, Shimane, 690-8504, Japan*

†Electronic supplementary information (ESI) available. CCDC 1996098 and 1996099. For ESI and crystallographic data in CIF or other electronic format see DOI: 10.1039/d0ob01213k

same number of electrons on six atoms. As pyridine-containing porphyrins, macrocycles bearing pyridine or 3-oxypyridine rings have been reported. Among them, pyridine rings without substituents at the β- or γ-positions favour aromaticity of 6π pyridine rings, with their macrocyclic aromaticity connected in a cross-conjugated manner.[6] In contrast, in molecules with 3-oxypyridine (pyridone) rings, macrocyclic 18π aromaticity takes priority over aromaticity of the 6π pyridine ring.[7] A similar system of 3-hydroxybenziporphyrins and the induction of aromaticity by deprotection of the methyl group were also reported.[8] From these previous research studies, the usage of the 3-oxypyridine ring can effectively induce aromaticity in expanded porphyrin macrocycles. Previously, Setsune *et al.* reported expanded porphyrins containing pyridine moieties in their structure, although these molecules did not show macrocyclic aromaticity.[9] Sessler *et al.* also reported the synthesis of cyclo[*m*]pyridine[*n*]pyrroles, which showed aromaticity only under acidic conditions.[10] In addition, pyrrole and pyridine moieties of **1** have been designed to prevent *meso*-carbon oxygenation.[11]

The synthetic procedure for **1** is shown in Scheme 2. To synthesise the desired 3-oxypyripentaphyrin(0.1.1.1.0), we designed the synthesis of a directly connected pyrrole–pyridine–pyrrole (dipyrropyridine) moiety known in the synthesis of expanded pyriporphyrins.[9a,12] Using the Miyaura–Ishiyama borylation, 2-ethoxycarbonyl-5-iodo-3,4-dimethylpyrrole **3** was transformed into a borylated analog **4** in 72% yield. Compound **4** (2 equiv.) was coupled with 2,6-diiodopyridin-3-ol to afford a new directly bonded pyrrole–pyridine–pyrrole trimer **5** in 61% yield. The hydroxyl group of **5** was protected with benzyl bromide to give benzyl ether **6** quantitatively. The terminal ethoxycarbonyl groups of **6** were completely hydrolysed by saponification affording **7** quantitatively. Without the protection of the hydroxyl group, the saponification of **5** produced a complex mixture and the corresponding carboxylic acid was not obtained at all. Through decarboxylation using NaOH and glycerol at 180 °C, dipyrropyridine **8** was obtained in 42% yield. Trimer **8** was condensed with pentafluorophenyl-substituted dipyrromethane dicarbinol **9′**, which was prepared from the reduction of acyl precursor **9**. Similarly to our reported procedure for the synthesis of pyripentaphyrin,[11] acid-catalysed condensation using *p*-toluenesulfonic acid (1.3 equiv.) followed by oxidation with 2,3-dichloro-5,6-dicyano-1,4-benzoquinone (DDQ; 3.0 equiv.) afforded benzyl-protected pyripentaphyrin(0.1.1.1.0) **1** in 19% yield. The benzyl group of **1** was intact under the oxidative conditions.

High-resolution electrospray ionization mass spectroscopy (HR-ESI-TOF-MS) provided the parent ion peak of **1** at m/z = 1036.2133 (calcd for 1036.2128). The ^{1}H NMR chemical shifts of **1** indicated its nonaromatic conjugation character, including the peaks of β protons at 6.41, 6.51, 6.75, and 6.80 ppm. In contrast, the peaks for pyridyl protons were observed at the downfield-shifted range (7.75 and 8.31 ppm), reflecting the electron-deficient aromatic 6π conjugation circuit of the pyridine ring. Inner NH protons were observed at 5.06 ppm, which seem to be derived from fast tautomeric exchange with protons of water in $CDCl_3$.[13]

The structure of **1** was unambiguously determined by X-ray crystallographic analysis.[14] The X-ray crystal structure was obtained in the protonated form with the counter chloride anion, as generated by 1,2-dichloroethane employed as the crystallisation solvent. In the X-ray crystal structure of the pyridine ring of **1**, the pyridine ring showed C–C bond lengths in the range of 1.386(6)–1.417(6) Å, which were typical of aromatic C–C bonds. The C–N bond lengths of the pyridine ring were 1.334(5) and 1.345(7) Å, indicating its aromatic character (Fig. 2b).

We conducted deprotection of the benzyl group of **1** using hydrogenation under Pd/C catalysis, which proceeded almost quantitatively (Scheme 2). Simple chromatographic separation followed by recrystallisation furnished **2** in 78% yield. HR-ESI-TOF-MS analysis of **2** showed a peak at m/z = 946.1691

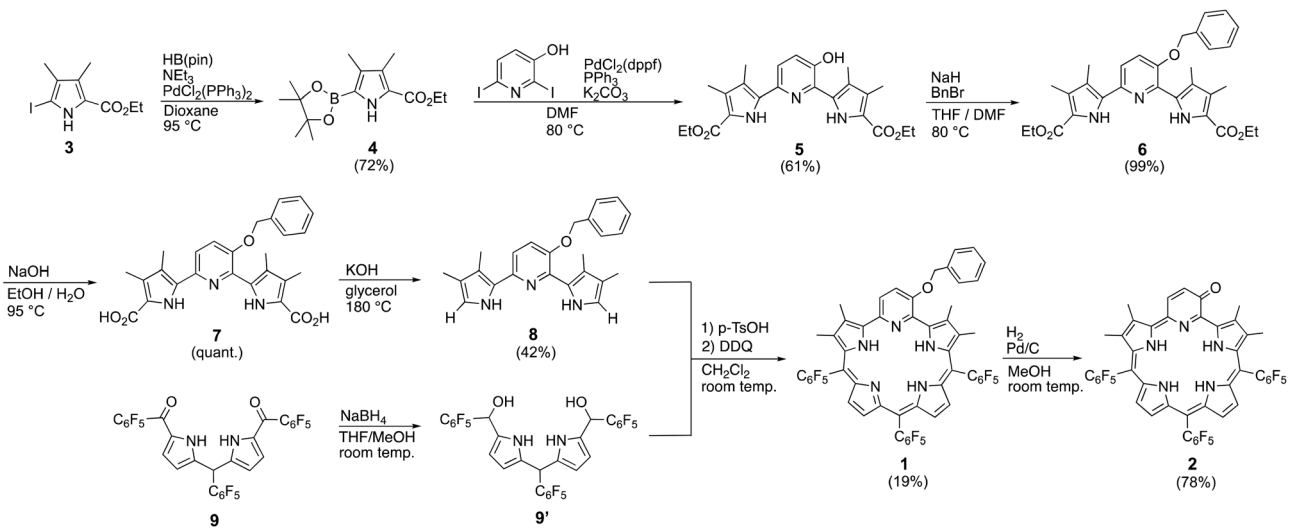

Scheme 2 Synthetic procedure of 3-oxypyripentaphyrins **1** and **2**.

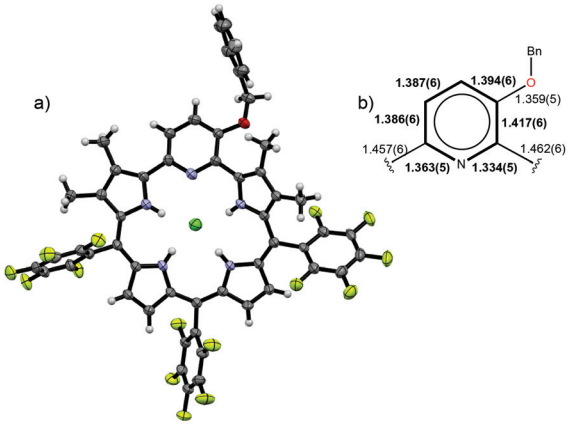

Fig. 2 X-ray crystal structure of 3-benzyloxypyripentaphyrin **1**·HCl. (a) Top view and (b) selected bond lengths of the pyridine unit shown in Å. Solvent molecules and *meso*-aryl groups in the side view were omitted. The thermal ellipsoids are shown at the 50% probability level.

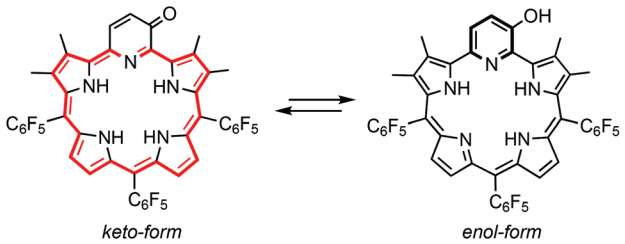

Scheme 3 Keto–enol tautomerisation of **2**.

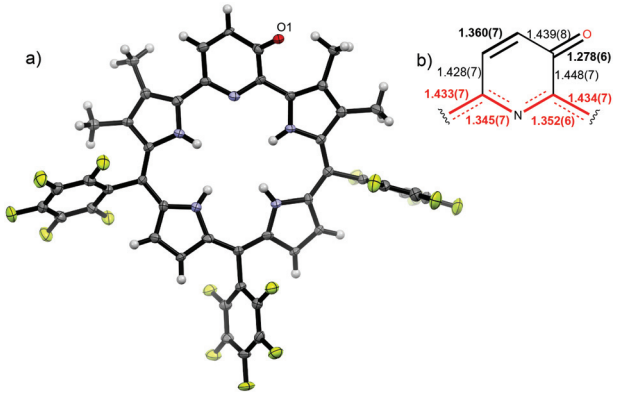

Fig. 3 X-ray crystal structure of 3-oxypyripentaphyrin **2**. (a) Top view and (b) selected bond lengths shown in Å. Solvent molecules and *meso*-aryl groups in the side view were omitted. The thermal ellipsoids are shown at the 50% probability level.

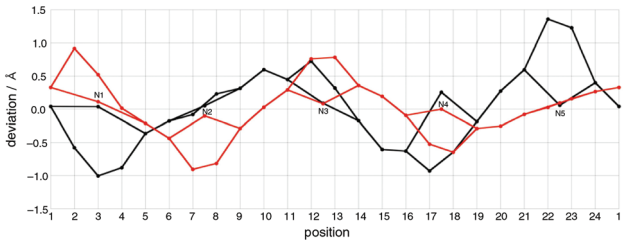

Fig. 4 Mean-plane deviation diagram calculated from the 29 core atoms for X-ray crystal structures of **1** (black) and **2** (red).

(calcd for $C_{46}H_{22}N_5F_{15}O_1$: 946.1663), which indicated the expected benzyl group removal. The NMR spectrum of **2** in $CDCl_3$ clearly showed downfield-shifted β-protons in the range of 7.8–8.2 ppm, although complete characterisation of them was not easy because of the broadened peaks (Fig. S13†). This broad NMR spectrum might be attributed to fast equilibrium of keto and enol forms of **2** (Scheme 3). The NMR peaks did not sharpen even at lower or higher temperature. However, in CD_3OD, highly downfield-shifted peaks belonging to pyrrole-β protons were clearly observed at 7.87–8.23 ppm, indicating the aromatic character. The peak for the β-proton of the 3-pyridone unit was highly downfield-shifted to 9.67 ppm owing to the diatropic ring current of the 22π conjugation circuit and the electron-withdrawing effect of the conjugated carbonyl group (Fig. S14†). These data support the increased contribution of the keto-form in protic solvents, as known in the tautomerism between the 4- and 2-pyridone derivatives.[15] The X-ray crystal structure of **2**[16] grown from the slow diffusion of hexane into chloroform solution was determined to be the keto-form with four amine-type pyrrolic nitrogen atoms (Fig. 3). All pyrrole and pyridone units were inward-pointing. The detailed X-ray crystallographic structure showed a C–O bond of 1.278(6) Å, indicating the strong double-bond character of **2**. In the 3-oxypyridine ring, the C–N bond lengths were 1.345(6) and 1.352(6) Å, indicating a retained aromatic bond character, while the bond-length alternation of the C–C bonds was larger than those of **1**, at 1.448(7), 1.439(8) and 1.428(7) Å for three single C–C bonds and 1.360(7) Å for one double C–C bond, suggesting the keto-form of **2** in the solid state. Furthermore, the pyridine–pyrrole C–C bond lengths were 1.434(7) and 1.433 (7) Å, which were shortened to the aromatic bond length region compared with those in **1** (1.462(6) and 1.457(6) Å). The harmonic oscillator model of aromaticity (HOMA)[17] value for the overall 22π macrocyclic structure of **2** was 0.71, which was larger than that of the cross-conjugated macrocyclic pathway of **1** calculated as 0.56 (Fig. S16†). The mean plane deviation (MPD) of the pentaphyrin skeleton of **2** was calculated as 0.33 Å suggesting a relatively planar structure of **2** than that of **1** with 0.46 Å of MPD (Fig. 4).

The aromaticity and strong NIR absorption of **2** were confirmed by its UV/Vis absorption spectra (Fig. 5). The absorption spectrum of **1** showed a relatively broad Soret-like band at 435 nm and almost no Q-like bands, suggesting its nonaromatic characteristics. However, **2** in dichloromethane showed a similar overall absorption spectrum shape, except for weak absorption bands at 437, 497, 519, 716 and 842 nm, which can be assigned to the 22π conjugation circuit. Furthermore, in methanol, all these peaks showed increased intensity, with a high molar coefficient observed. In particular, the strong Q-like absorption band at 852 nm with an absorption coeffi-

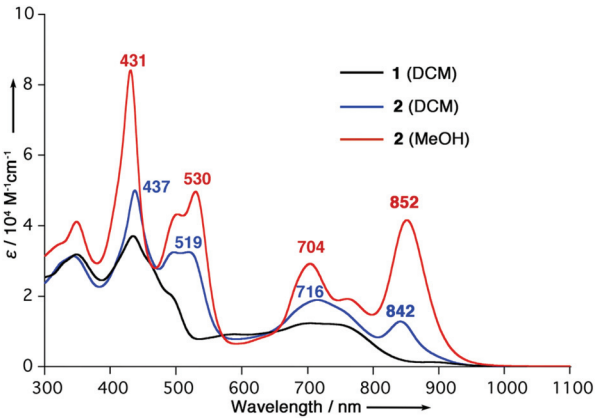

Fig. 5 UV/Vis absorption spectra of **1** in dichloromethane (black) and **2** in dichloromethane (blue) and **2** in methanol (red).

cient of 4.2×10^4 M^{-1} cm^{-1} suggested the suitability of this compound as a NIR photosensitiser.

To investigate the aromaticity of **2**, we conducted DFT calculation[18] (B3LYP/6-31G level) on the keto and enol forms of **2**. The aromaticity of the keto-form of **2** was supported by the calculated nucleus-independent chemical shift (NICS(0)) value[19] of −10.91 ppm at the gravity point of the macrocycle. In contrast, those of **1** and the enol-form of **2** were calculated to be −0.66 and −0.73 ppm, respectively, indicating a nonaromatic character. Meanwhile, the NICS(0) values of the six-membered ring in **1** and the enol-form of **2** were −9.73 and −9.98 ppm, respectively, owing to their 6π-electron aromaticity, while that of the keto-form of **2** was +4.08 ppm because the point was not the centre of a 6π ring but the outside periphery of a 22π macrocycle. The keto-form of **2** was slightly (16.7 kJ mol^{-1}) more stable than the enol-form though the HOMO–LUMO gaps of **1** and the keto and enol forms of **2** were very similar (1.97–2.00 eV), as observed in cyclic voltammograms with similar HOMO–LUMO gaps of **1** and **2** (1.45–1.40 eV, see the ESI†).

In conclusion, we have synthesised benzyl-group-protected pyripentaphyrin **1** and demonstrated its deprotection using hydrogenation to produce 3-oxypyripentaphyrin **2**. The transformation from nonaromatic **1** into aromatic **2** drastically induced aromaticity in the 22π conjugation system, preserving its stability. The aromaticity of **2** was enhanced in methanol, with strong NIR absorption observed. Therefore, we have demonstrated the potential of expanded pyriporphyrins as theoretically promising photosensitizer candidates.

Conflicts of interest

There are no conflicts to declare.

Acknowledgements

This work was supported by a JSPS KAKENHI grant for young scientists no. 17K14445(B) from the MEXT of Japan and the Inohana Foundation.

Notes and references

1 (*a*) D. Dolmans, D. Fukumura and R. K. Jain, *Nat. Rev. Cancer*, 2003, **3**, 380–387; (*b*) J. Zhang, C. Jiang, J. P. F. Longo, R. B. Azevedo, H. Zhang and L. A. Muehlmann, *Acta Pharm. Sin. B*, 2018, **8**, 137–146; (*c*) J. Kou, D. Dou and L. Yang, *Oncotarget*, 2017, **8**, 81591–81603.

2 (*a*) N. M. Idris, M. K. Gnanasammandhan, J. Zhang, P. C. Ho, R. Mahendran and Y. Zhang, *Nat. Med.*, 2012, **18**, 1580–1585; (*b*) J. M. Frangioni, *Curr. Opin. Chem. Biol.*, 2003, **7**, 626–634.

3 (*a*) J. L. Sessler and D. Seidel, *Angew. Chem., Int. Ed.*, 2003, **42**, 5134–5175; (*b*) T. K. Chandrashekar and S. Venkatraman, *Acc. Chem. Res.*, 2003, **36**, 676–691; (*c*) M. Stepien, N. Sprutta and L. Latos-Grażyński, *Angew. Chem., Int. Ed.*, 2011, **50**, 4288–4340; (*d*) S. Saito and A. Osuka, *Angew. Chem., Int. Ed.*, 2011, **50**, 4342–4373; (*e*) T. Tanaka and A. Osuka, *Chem. Rev.*, 2017, **117**, 2584–2640; (*f*) B. Szyszko, M. J. Białek, E. Pacholska-Dudziak and L. Latos-Grażyński, *Chem. Rev.*, 2017, **117**, 2839–2909; (*g*) T. Chatterjee, A. Srinivasan, M. Ravikanth and T. K. Chandrashekar, *Chem. Rev.*, 2017, **117**, 3329–3376.

4 (*a*) J. L. Sessler, N. A. Tvermoes, J. Davis, P. Anzenbacher Jr., K. Jursícová, W. Sato, D. Seidel, V. Lynch, C. B. Black, A. Try, B. Andrioletti, G. Hemmi, T. D. Mody, D. J. Magda and V. Král, *Pure Appl. Chem.*, 1999, 2009–2018; (*b*) C. Comuzzi, S. Cogoi, M. Overhand, G. A. V. Marel, H. S. Overleeft and L. E. Xodo, *J. Med. Chem.*, 2006, **49**, 196–204; (*c*) C. S. Gutsche, M. Ortwerth, S. Gräfe, K. J. Flanagan, M. O. Senge, H.-U. Reissig, N. Kulak and A. Wiehe, *Chem. – Eur. J.*, 2016, **22**, 13953–13964.

5 (*a*) J. L. Sessler, J. M. Davis and V. Lynch, *J. Org. Chem.*, 1998, **63**, 7062–7065; (*b*) J. L. Sessler, D. Seidel, C. Bucher and V. Lynch, *Tetrahedron*, 2001, **57**, 3743–3752; (*c*) Z. S. Yoon, D.-G. Cho, K. S. Kim, J. L. Sessler and D. Kim, *J. Am. Chem. Soc.*, 2008, **130**, 6930–6931.

6 (*a*) K. Berlin and E. Breitmaier, *Angew. Chem., Int. Ed. Engl.*, 1994, **33**, 219–220; (*b*) R. Myśliborski, L. Latos-Grażyński and L. Szterenberg, *Eur. J. Org. Chem.*, 2006, 3064–3068.

7 (*a*) T. D. Lash and S. T. Chaney, *Chem. – Eur. J.*, 1996, **2**, 944–948; (*b*) T. Shrönemeier and E. Breitmaier, *Synthesis*, 1997, 273; (*c*) T. D. Lash, S. T. Chaney and D. T. Richter, *J. Org. Chem.*, 1998, **63**, 9076–9088; (*d*) D. Liu, G. M. Ferrence and T. D. Lash, *J. Org. Chem.*, 2004, **69**, 6079–6093; (*e*) T. D. Lash, K. P. Pokharel, J. M. Serling, V. R. Yant and G. M. Ferrence, *Org. Lett.*, 2007, **9**, 2863–2866; (*f*) S. Neya, M. Suzuki, H. Ode, T. Hoshino, Y. Furutani, H. Kandori, H. Hori, K. Imai and T. Komatsu, *Inorg. Chem.*, 2008, **47**, 10771–10778; (*g*) S. Neya, M. Suzuki, T. Mochizuki, T. Hoshino and A. T. Kawaguchi, *Eur. J. Org. Chem.*, 2015, 3824–3829.

8 D. T. Richter and T. D. Lash, *Tetrahedron*, 2001, **57**, 3657–3671.

9 (*a*) J.-I. Setsune and K. Watanabe, *J. Am. Chem. Soc.*, 2008, **130**, 2404–2405; (*b*) J.-I. Setsune and K. Yamato, *Chem. Commun.*, 2012, **48**, 4447–4449.

10 (*a*) Z. Zhang, J. M. Lim, M. Ishida, V. V. Roznyatovsky, V. M. Lynch, H.-Y. Gong, X. Yang, D. Kim and J. L. Sessler, *J. Am. Chem. Soc.*, 2012, **134**, 4076–4079; (*b*) Z. Chang, W.-Y. Cha, N. J. Williams, E. L. Rush, M. Ishida, V. M. Lynch, D. Kim and J. L. Sessler, *J. Am. Chem. Soc.*, 2014, **136**, 7591–7594.

11 D. Mori, T. Yoneda, M. Suzuki, T. Hoshino and S. Neya, *Chem. – Asian J.*, 2019, **14**, 4169–4173.

12 J.-I. Setsune, M. Toda, K. Watanabe, P. K. Panda and T. Yoshida, *Tetrahedron Lett.*, 2006, **47**, 7541–7544.

13 K. Rachlewicz, L. Latos-Grażyński, A. Hebauer, A. Vivian and J. L. Sessler, *J. Chem. Soc., Perkin Trans. 2*, 1999, 2189–2195.

14 X-ray data for **1**·HCl: $(C_{53}H_{29}F_{15}N_5O_1)$·HCl·2(1,2-dichloroethane) (Mr = 1171.22), triclinic, space group $P\bar{1}$ (no. 2), a = 13.2433(3), b = 13.7134(3), c = 15.7312(4) Å, α = 70.848(1)°, β = 80.596(1)°, γ = 66.090(1)°, V = 2465.69(10) Å^3, Z = 2, ρ_{calcd} = 1.577 g cm^{-3}, T = 93(2) K, R_1 = 0.0841 ($I > 2\sigma(I)$), wR_2 = 0.2495 (all data), GOF = 1.120. CCDC 1996098† contains the supplementary crystallographic data for this paper.

15 A. Gordon and A. R. Katritzky, *Tetrahedron Lett.*, 1968, **23**, 2767–2770.

16 X-ray data for **2**: $(C_{46}H_{22}F_{15}N_5O_1)$·2(chloroform) (Mr = 1184.42), monoclinic, space group $P\bar{1}$ (no. 2), a = 12.2776 (3), b = 13.0559(3), c = 16.5083(4) Å, α = 105.241(1)°, β = 110.613(1)°, γ = 98.939(2)°, V = 2297.85(10) Å^3, Z = 2, ρ_{calcd} = 1.712 g cm^{-3}, T = 93(2) K, R_1 = 0.0965 ($I > 2\sigma(I)$), wR_2 = 0.2705 (all data), GOF = 0.1049. CCDC 1996099† contains the supplementary crystallographic data for this paper.

17 (*a*) T. M. Krygowski and T. M. Cryański, *Tetrahedron*, 1996, **52**, 1713–1722; (*b*) T. M. Krygowski and T. M. Cryański, *Tetrahedron*, 1996, **52**, 10255–10264.

18 M. J. Frisch, *et al.*, *Gaussian 09, Revision A.02*, Gaussian, Inc., Wallingford, CT, 2009, (full citation in the ESI†).

19 (*a*) P. V. R. Schleyer, C. Maerker, A. Dransfeld, H. Jiao and N. J. R. V. E. Hommes, *J. Am. Chem. Soc.*, 1996, **118**, 6317–6318; (*b*) Z. Chen, C. S. Wannere, C. Corminboeuf, R. T. Puchta and P. V. R. Schleyer, *Chem. Rev.*, 2005, **105**, 3842–3888.

